Proceedings of the
46th IEEE Conference on Decision and Control
New Orleans, LA, USA, Dec. 12-14, 2007

A comparison between Zernike and PCA representation of atmospheric turbulence

Alessandro Beghi, Angelo Cenedese, and Andrea Masiero

Abstract— **In ground-based astronomy seeing remains one of the biggest problem due to the presence of atmospheric turbulence affecting the radiation from the astronomical object of interest, along its travel path to the telescope device. The correction of the turbulence effects at the telescope pupil level, characterized statistically according to well-accepted models, is the focus of current generation of adaptive optics systems. Moreover, the representation of atmospheric turbulence, which is limited to the phase contribution since the amplitude degradation can be considered as negligible, is obtained through a modal decomposition. The choice of the modal representation is therefore a key issue in the turbulence study and the consequent design of control system to drive the deformation of the corrective mirrors. In the paper we discuss a possible solution to the problem, resorting to the Principal Component Analysis of the atmospheric turbulence, and comparing this approach to the classically adopted Zernike's expansion.**

I. INTRODUCTION

Nowadays, the exploration of the remote outer space and the study of astronomical objects is strongly relying on observations made by ground based telescopes, be they optical, radio, or other spectrum range telescopes. In particular, restricting the interest to the category of optical telescopes, researchers are facing the problem that seeing is one of the biggest problems for ground-based astronomy, up to the point that we refer to "astronomical seeing" as to the presence of blurring and loss of sharpness in images of astronomical objects, mainly due to the effect of turbulence in the atmosphere [1]. In actual fact, without resorting to additional corrections, the theoretical resolution of big telescopes is hugely degraded by the turbulence encountered along the line of sight of the device, resulting in images of scantly defined objects with presence of speckles.

As far as the description of the atmosphere is concerned, some considerations are in order.
Firstly, due to the intrinsic stochasticity of the turbulence, the modelling of these atmospheric phenomena is based on statistical models. Assuming the turbulence to be stationary the spatial characteristics of the turbulence are temporally invariant: the Von Karman model of turbulence spatial characteristics will be described in Section II.

This work forms part of the ELT Design Study and is supported by the European Commission, within Framework Programme 6, contract No 011863.

A.Beghi and A.Masiero are with the Dipartimento di Ingegneria dell'Informazione, Università di Padova, via Gradenigo 6/B, 35131 Padova, Italy {beghi,masiero}@dei.unipd.it

A.Cenedese is with the Dipartimento di Tecnica e Gestione dei Sistemi Industriali, Università di Padova, Stradella San Nicola 3, 36100 Vicenza, Italy angelo.cenedese@unipd.it

Secondly, given a certain light source (the object to be observed) characterized with an emission point spread function P_0, due to the presence of turbulence, the detected P appears as degraded with respect to the ideal P_0, and the degradation is related to the varying of the refraction index that leads directly to phase fluctuations while amplitude variations are brought in as a second-order effect and negligibly affect the imaging performance. In this sense, we will consider turbulent phase only.
Finally, there is the need of discretization. The atmosphere is a continuum, and it is affecting the phase of the radiation emitted by the object of interest with continuity along the path travelled by the radiation. To simplify the study, the turbulence is generally modeled as a superposition of a finite number l of layers: the i^{th} layer models the atmosphere from h_{i-1} to h_i meter high, where $h_0 = 0$, as in Fig. 1(a). Each layer is assumed to translate in front of the telescope pupil with constant velocity. Moreover each layer is considered to be independent on the others, hence the overall turbulence can be taken as a linear combination of single layers effect. Finally, not only is the turbulence discretized into layers, but also it is described according to a generalized modal representation. The wavefront phase $\Phi(r)$ can be expressed as a polynomial expansion, by means of a Zernike's base. Quoting from [2]: *The Zernike polynomials $Z_j(r, \theta)$ are an orthogonal expansion over the unit circle, and have a long tradition of use in classical optical aberration analysis. They have been adopted by the AO community as the* de facto *standard rightly or wrongly (probably the latter).*

This aspect is considered in more detail in Section IV and raises the issues of studying an alternative approach to represent the atmospheric turbulence, as done in this work resorting to the Principal Component Analysis (PCA) approach and presented in comparison with the Zernike's model in Section V.

Astronomers have already considered the use of Karhunen-Loève bases to represent the turbulent phase: Since the coefficients of Karhunen-Loève transform are uncorrelated, they provide an optimal set of bases in the continuous spatial domain. However the computation of Karhunen-Loève coefficients is done indirectly: First a finite set of Zernike coefficients are computed and then Karhunen-Loève bases are approximated by the matrix that diagonalize the Zernike coefficients covariance matrix. Since this procedure can be quite long and gives only an approximated result, we propose to solve the problem on the discrete domain given by the wavefront sensors. Indeed in this discrete domain we can compute the optimal bases using principal component

1-4244-1498-9/07/$25.00 ©2007 IEEE.

analysis.

II. TURBULENCE STATISTICAL MODEL

In this paper we consider a comparison between Zernike and PCA bases for the spatial representation of the turbulence: Since the spatial characteristics of the turbulence are assumed to be invariant, then we consider the time as fixed at a constant value $t = \bar{t}$. Furthermore to simplify the notation we will omit $\bar{t}$ from equations.

Let $\phi(r_i)$ be the value of the turbulent phase at the point r_i on the aperture plane. Considering the turbulent phase as a spatial process, it is usually assumed to be a zero-mean (wide-sense) stationary stochastic process: Thus it is completely characterized by its second order properties. Its spatial statistical model is commonly described by means of the structure function, which measures the averaged difference between the phase at two points at locations r_1 and r_2 of the wavefront (see Fig. 1(b)), which are separated by a distance r,

$$D_\phi(r) = \left\langle |\phi(r_1) - \phi(r_2)|^2 \right\rangle .$$

The structure function D_ϕ is related to the covariance function $C_\phi(r) = \langle \phi(r_1), \phi(r_2) \rangle$, as:

$$D_\phi(r) = 2\left(\sigma_\phi^2 - C_\phi(r)\right), \tag{1}$$

where σ_ϕ^2 is the phase variance.

According to the Von Karman theory, the phase structure function evaluated at distance r is the following [4]:

$$D_\phi(r) = \left(\frac{L_0}{r_0}\right)^{5/3} c \left[\frac{\Gamma(5/6)}{2^{1/6}} - \left(\frac{2\pi r}{L_0}\right)^{5/6} K_{5/6}\left(\frac{2\pi r}{L_0}\right)\right],$$

where $K_\cdot(\cdot)$ is the MacDonald function (modified Bessel function of the third type), Γ is the Gamma function, L_0 is the outer scale, r_0 is a characteristic parameter called the Fried parameter [6], and c is a suitable constant [1].

From the relation between the structure function and the covariance (1), the spatial covariance of the phase between two points at distance r results

$$C_\phi(r) = \left(\frac{L_0}{r_0}\right)^{5/3} \frac{c}{2} \left(\frac{2\pi r}{L_0}\right)^{5/6} \mathrm{K}_{5/6}\left(\frac{2\pi r}{L_0}\right). \tag{2}$$

III. PHASE RECONSTRUCTION

In this section we introduce a statistical model for the measurement procedure. Exploiting this statistical model we shall be able to compare performances of different types of turbulence representations. In particular we will compare the performances of Zernike polynomials, which are probably the most used set of bases for turbulent phase representation, with those of PCA bases. These will be briefly reviewed respectively in Section IV-A and IV-B.

Fig. 1(b) shows the domain of images formed on the telescope lens. Since equations derived considering the simplified domain of Fig. 1(c) can easily be extended to the case

[1]That is $c = \frac{2^{1/6}\Gamma(11/6)}{\pi^{8/3}} \left[\frac{24}{5}\Gamma(6/5)\right]^{5/6}$.

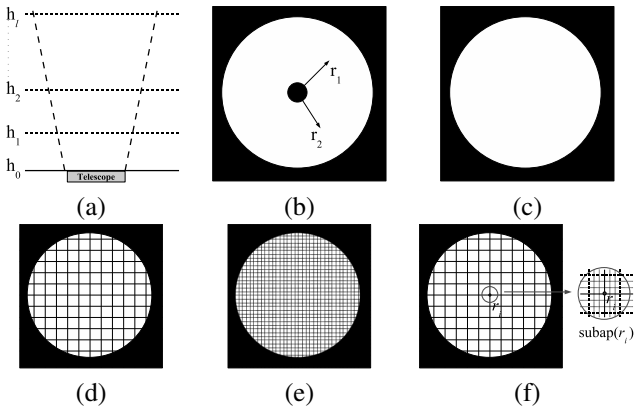

Fig. 1. (a) Atmospheric turbulence is modeled as a superposition of l layers. (b) Telescope image domain and coordinates. (c) Telescope image simplified domain. (d) Continuous line grid: domain $\mathbb{L}$. (e) Dashed line grid: domain $\mathbb{L}_{sp}$. (f) Example of subaperture.

of Fig. 1(b), we neglect the central hole of the telescope, thus we concentrate on the case of Fig. 1(c).

In real applications only a finite number of sensors is available: These are usually distributed on a grid, thus the turbulent phase is measured only on a discrete domain $\mathbb{L}$, which is that in Fig. 1(d), i.e. a sensor is placed at each node of the grid. Without loss of generality we assume that sensors are uniformly spaced: The closest neighbors of each sensor (both along the horizontal and the vertical directions) are placed at a distance of p_s meters.

To reduce noise influence on the measurements, sensor at point r_i usually takes some kind of spatial mean of the turbulent phase among its neighborhood. We call *subaperture* corresponding to r_i, the set of points considered by the sensor placed on r_i to take its measurement. To be more precise, first let $\mathbb{L}_{sp}$ be the grid of Fig. 1(e), then $\mathbb{L}_{sp}$ is decomposed in $|\mathbb{L}|$ subsets, which are the subapertures: The subaperture corresponding to $r_i \in \mathbb{L}$ is

$$\text{subap}(r_i) = \left\{ r_j \in \mathbb{L}_{sp} \mid r_i = \arg\min_{r_{i^*} \in \mathbb{L}} ||r_{i^*} - r_j||^2 \right\}.$$

According to the above definition, subapertures are disjoint sets. An example of subaperture is the set of nodes inside the square in bold dashed line in Fig. 1(f).

With an abuse of notation let ϕ and $\bar{\phi}$ be the vectors containing the turbulent phase values respectively on $\mathbb{L}$ and on $\mathbb{L}_{sp}$. Notice that $\mathbb{L} \subset \mathbb{L}_{sp}$, thus for each i, $1 \le i \le |\mathbb{L}|$, there exists a j, $1 \le j \le |\mathbb{L}_{sp}|$, such that ϕ_i, the i^{th} component of ϕ, is equal to $\bar{\phi}_j$, the j^{th} component of $\bar{\phi}$. Thus we can define

$$W(i,j) = \begin{cases} 1 & \text{if } \phi_i = \bar{\phi}_j \\ 0 & \text{otherwise.} \end{cases}$$

such that $\phi = W\bar{\phi}$.

First notice that the adaptive optics system doesn't take into consideration the phase translation over the entire telescope aperture: Thus we will neglect the current mean of the

signal. Hence the aim is to estimate φ, defined as follows

$$\begin{aligned}\varphi &= W\bar{\phi} - \frac{1}{|\mathbb{L}|}\begin{bmatrix}1\\ \vdots \\ 1\end{bmatrix}\left(\begin{bmatrix}1 & \dots & 1\end{bmatrix} W\bar{\phi}\right)\\ &= \left(I - \frac{1}{|\mathbb{L}|}\mathbf{1}\right) W\bar{\phi}\end{aligned}$$

where $\mathbf{1}$ is a $|\mathbb{L}| \times |\mathbb{L}||$ matrix of ones.

We assume that the measurement process is linear: That is the measurement vector y is in fact given by a linear combination of $\bar{\phi}$, eventually affected by noise

$$y = H\ \bar{\phi} + w$$

where H is the measurement matrix and w is the noise process. Even if there are several types of noise which can occur in the measurement process, we shall assume that their global effect, w, is a zero-mean Gaussian noise, i.e. $w \sim \mathcal{N}(0, \Sigma_w)$. Usually $\Sigma_w = I\sigma_w^2$. Moreover we assume $w(t)$ uncorrelated with $\phi(t')\ \forall t'$ and with $w(t')\ \forall t' \neq t$.

Since we cannot access directly to the value of φ, we use the measurement vector y to estimate it. Let $\bar{\varphi}(y)$ indicate the best, minimum variance, linear estimator of φ using y. Let $\Sigma_{\bar{\phi}}$, Σ_y, $\Sigma_{\varphi y}$ be defined as follows:

$$\begin{aligned}\Sigma_{\bar{\phi}} &= \mathbf{E}[\bar{\phi}\bar{\phi}^T]\\ \Sigma_y &= \mathbf{E}[yy^T] = H\Sigma_{\bar{\phi}}H^T + \Sigma_w\\ \Sigma_{\varphi y} &= \mathbf{E}[\varphi y^T] = \left(I - \tfrac{1}{|\mathbb{L}|}\mathbf{1}\right) W\Sigma_{\bar{\phi}}H^T\\ \Sigma_\varphi &= \mathbf{E}[\varphi\varphi^T] = \left(I - \tfrac{1}{|\mathbb{L}|}\mathbf{1}\right) W\Sigma_{\bar{\phi}}W^T\left(I - \tfrac{1}{|\mathbb{L}|}\mathbf{1}\right)^T.\end{aligned}$$

The covariance matrix $\Sigma_{\bar{\phi}}$ can be computed from (2) as follows:

$$\Sigma_{\bar{\phi}} = \begin{bmatrix} \Sigma(1,1) & \dots & \dots & \dots & \dots \\ \Sigma(2,1) & \dots & \dots & \dots & \dots \\ \dots & \dots & \dots & \dots & \dots \\ \Sigma(i,1) & \dots & \Sigma(i,j) & \Sigma(i,j+1) & \dots \\ \Sigma(i+1,1) & \dots & \Sigma(i+1,j) & \dots & \dots \\ \dots & \dots & \dots & \dots & \dots \end{bmatrix}$$

where

$$\begin{aligned}\Sigma(i,j) = \mathbf{E}[\bar{\phi}(i)\bar{\phi}(j)] &= \mathbf{E}\left[\phi(r_i)\phi(r_j)\right]\\ &= C_\phi(|r_i - r_j|). \qquad (3)\end{aligned}$$

Then

$$\bar{\varphi}(y) = \Sigma_{\varphi y}\Sigma_y^{-1}y$$

and substituting the explicit expressions for $\Sigma_{\varphi y}$ and Σ_y^{-1}:

$$\bar{\varphi}(y) = \left(I - \frac{1}{|\mathbb{L}|}\mathbf{1}\right) W\Sigma_{\bar{\phi}}H^T\left(H\Sigma_{\bar{\phi}}H^T + \Sigma_w\right)^{-1}y \quad (4)$$

where we used the a priori statistical information about $\bar{\phi}$ (and thus also about φ).

In our simulation we consider two cases for the measurement process:

1) The measurement process of $\phi(r'_i)$ is modeled as a spatial mean on the subaperture corresponding to r'_i (Fig. 1(f) and Fig. 2(a)), that is:

$$\phi(r'_i) \approx \left(\sum_{r_j \in \text{subap}(r'_i)} \bar{\phi}(j)\right) \frac{1}{|\text{subap}(r'_i)|}.$$

Accordingly with the above equation, H is

$$H(i,j) = \begin{cases} \frac{1}{|\text{subap}(r'_i)|} & \text{if } r_j \in \text{subap}(r'_i) \\ 0 & \text{otherwise.}\end{cases}.$$

2) In this case we simulate the *Shack-Hartmann* sensor: It measures the values of phase's vertical and horizontal slopes instead of measuring the phase itself. Let the sets $I_1(r'_i)$, $I_2(r'_i)$, $I_3(r'_i)$, $I_4(r'_i)$ be defined as follows

$$I_1(r'_i) = \{r_j \in \mathbb{L}_{sp} \mid r_j \in \text{subap}(r'_i),\ r_j \text{ is in the top row of subap}(r'_i)\}$$

$$I_2(r'_i) = \{r_j \in \mathbb{L}_{sp} \mid r_j \in \text{subap}(r'_i),\ r_j \text{ is in the bottom row of subap}(r'_i)\}$$

$$I_3(r'_i) = \{r_j \in \mathbb{L}_{sp} \mid r_j \in \text{subap}(r'_i),\ r_j \text{ is in the left-border column of subap}(r'_i)\}$$

$$I_4(r'_i) = \{r_j \in \mathbb{L}_{sp} \mid r_j \in \text{subap}(r'_i),\ r_j \text{ is in the right-border column of subap}(r'_i)\}$$

$I_1(r'_i)$, $I_2(r'_i)$, $I_3(r'_i)$, $I_4(r'_i)$ are also shown in Fig. 2(b) and Fig. 2(c). Then the measurement procedure is assumed to be *quadcell*-like: Vertical and horizontal slopes at r'_i (which are indicated respectively with $d_v(r'_i)$ and $d_h(r'_i)$) are approximated by:

$$\begin{aligned}d_v(r'_i) &\approx \sum_{r_j \in I_1(r'_i)} \frac{\bar{\phi}(j)}{|I_1(r'_i)|} - \sum_{r_j \in I_2(r'_i)} \frac{\bar{\phi}(j)}{|I_2(r'_i)|}\\ d_h(r'_i) &\approx \sum_{r_j \in I_3(r'_i)} \frac{\bar{\phi}(j)}{|I_3(r'_i)|} - \sum_{r_j \in I_4(r'_i)} \frac{\bar{\phi}(j)}{|I_4(r'_i)|}.\end{aligned}$$

Thus two measurements are available for each r'_i, corresponding to the estimates of $d_v(r'_i)$ and $d_h(r'_i)$. Let

$$H_1(i,j) = \begin{cases} \frac{1}{|I_1(r'_i)|} & \text{if } r_j \in I_1(r'_i) \\ -\frac{1}{|I_2(r'_i)|} & \text{if } r_j \in I_2(r'_i) \\ 0 & \text{otherwise}\end{cases}$$

$$H_2(i,j) = \begin{cases} \frac{1}{|I_3(r'_i)|} & \text{if } r_j \in I_3(r'_i) \\ -\frac{1}{|I_4(r'_i)|} & \text{if } r_j \in I_4(r'_i) \\ 0 & \text{otherwise}\end{cases}$$

then H is

$$H = \begin{bmatrix} H_1 \\ H_2 \end{bmatrix}.$$

Notice that also some other similar statistical models for the Shack-Hartmann sensor have been considered in the literature [9] [5].

Fig. 2. (a) Spatial mean on the subaperture corresponding to r_i. (b) Shack-Hartmann's vertical slope estimation. (c) Shack-Hartmann's horizontal slope estimation.

Finally we define the (input) signal to noise ratio as follows: $SNR = \text{trace}(H\Sigma_{\bar{\phi}}H^T)/\text{trace}(\Sigma_w)$.

Since usually $|\mathbb{L}|$ is quite large, a dimensional reduction step is commonly introduced to reduce both running time and required storage memory. Instead of using the canonical basis of $\mathbb{R}^{|\mathbb{L}|}$, a new set of bases $\bar{C}$ is introduced to represent $\varphi : \bar{C}$ should be chosen such that most of signal's energy is in fact concentrated in its first $N+1$ bases. Hence the dimensionality reduction step is performed discarding the last $|\mathbb{L}| - N - 1$ bases of $\bar{C}$. Depending on the chosen $\bar{C}$ the represented signal will be more or less close to the real one.

Assume that the column vectors $c_0, c_1, \ldots, c_{|\mathbb{L}|-1}$ form a basis of $\mathbb{R}^{|\mathbb{L}|}$ thus we can write

$$\bar{C} = \left[\begin{array}{cccc} c_0 & c_1 & \ldots & c_{|\mathbb{L}|-1} \end{array} \right] .$$

Then a generic vector $\bar{\phi} \in \mathbb{R}^{\mathbb{L}}$ can be represented as $\bar{\phi} = \sum_{i=0}^{|\mathbb{L}|-1} c_i a_i$ where a_i, $i = 0, \ldots, |\mathbb{L}| - 1$ are suitable coefficients.

Without loss of generality we will assume $c_0 = \left[\begin{array}{ccc} 1 & \ldots & 1 \end{array} \right]^T$ and $c_i \perp c_j$, $i = 1, \ldots, N$, $j = N+1, \ldots, |\mathbb{L}| - 1$. Both φ and $\bar{\varphi}(y)$ are orthogonal to c_0, i.e. $\varphi \in \text{span}\{c_1, \ldots, c_{|\mathbb{L}|-1}\}$ and $\bar{\varphi}(y) \in \text{span}\{c_1, \ldots, c_{|\mathbb{L}|-1}\}$. Thus there exist $a_1, \ldots, a_{|\mathbb{L}|-1}$ and $\hat{a}_1, \ldots, \hat{a}_{|\mathbb{L}|-1}$ such that

$$\varphi = \sum_{i=1}^{|\mathbb{L}|-1} c_i a_i = \left[\begin{array}{cc} C & C_b \end{array} \right] \left[\begin{array}{c} a \\ b \end{array} \right]$$

and

$$\bar{\varphi}(y) = \sum_{i=1}^{|\mathbb{L}|-1} c_i \hat{a}_i = \left[\begin{array}{cc} C & C_b \end{array} \right] \left[\begin{array}{c} \hat{a} \\ \hat{b} \end{array} \right]$$

where $C = \left[\begin{array}{ccc} c_1 \ldots c_N \end{array} \right]$, $C_b = \left[\begin{array}{ccc} c_{N+1} \ldots c_{|\mathbb{L}|-1} \end{array} \right]$ and $a = \left[\begin{array}{ccc} a_1 \ldots a_N \end{array} \right]^T$, $\hat{a} = \left[\begin{array}{ccc} \hat{a}_1 \ldots \hat{a}_N \end{array} \right]^T$, $b = \left[\begin{array}{ccc} a_{N+1} \ldots a_{|\mathbb{L}|-1} \end{array} \right]^T$, $\hat{b} = \left[\begin{array}{ccc} \hat{a}_{N+1} \ldots \hat{a}_{|\mathbb{L}|-1} \end{array} \right]^T$. Define $\hat{\varphi}(y)$ as the closest vector to $\bar{\varphi}(y)$ such that $\hat{\varphi}(y) \in \text{span}\{c_1, \ldots, c_N\}$. Then

$$\hat{\varphi}(y) = \sum_{i=0}^{N} c_i \hat{a}_i = C\hat{a} \tag{5}$$

with

$$\hat{a} = (C^T C)^{-1} C^T \bar{\varphi}(y) \ . \tag{6}$$

Let $C^\dagger$ be the pseudo-inverse of C, i.e. $C^\dagger = (C^T C)^{-1} C^T$. Then $\hat{a} = C^\dagger \bar{\varphi}(y)$.

If $\bar{C}$ is such that most of the energy of the signal is concentrated on its first bases then $\bar{\varphi}(y) \approx \hat{\varphi}(y)$.

Finally the relation between $\hat{\varphi}(y)$ and y can be summarized with

$$\hat{\varphi}(y) = C^\dagger \Sigma_{\varphi y} \Sigma_y^{-1} y = C\hat{a} = CFy \tag{7}$$

where

$$\hat{a} = Fy \tag{8}$$

and

$$F = C^\dagger \left(I - \frac{1}{|\mathbb{L}|}\mathbf{1} \right) W \Sigma_{\bar{\phi}} H^T \left(H \Sigma_{\bar{\phi}} H^T + \Sigma_w \right)^{-1} \ .$$

Let $\tilde{a} = a - \hat{a}$ and $\eta = C_b b$, then the *representation error* e, due both to considering only N bases instead of $|\mathbb{L}|$ and to noise, can be computed as follows:

$$e = \varphi - \hat{\varphi}(y) = Ca + C_b b - C\hat{a} = C\tilde{a} + \eta \ .$$

Since η depends only on the chosen set of bases and on the signal statistical characteristics we will call it *projection error*. Notice that a, $\hat{a}$, b, η and e are all zero mean processes. Moreover the columns of C are orthogonal to the column of C_b. Hence

$$\Sigma_e = \mathbf{E}[ee^T] = C\mathbf{E}[\tilde{a}\tilde{a}^T]C^T + \mathbf{E}[\eta\eta^T] = C\Sigma_{\tilde{a}}C^T + \Sigma_\eta$$

where $\Sigma_{\tilde{a}} = \mathbf{E}[\tilde{a}\tilde{a}^T] = C^\dagger \Sigma_\varphi (C^\dagger)^T - F\Sigma_y F^T$ and $\Sigma_\eta = \mathbf{E}[\eta\eta^T] = \Sigma_\varphi - CC^\dagger \Sigma_\varphi (C^\dagger)^T C^T$.

Finally we have

$$\mathbf{E}[\|e\|^2] = \mathbf{E}[e^T e] = \text{trace}(\Sigma_e). \tag{9}$$

Hence $\bar{C}$ should be chosen such that $\text{trace}(\Sigma_e)$ would be as small as possible even using few bases, i.e. when N is small.

IV. TURBULENCE REPRESENTATIONS

A. Zernike representation

Zernike polynomials are commonly used to represent signals defined inside a circle: This makes them particularly well suited to represent the turbulent phase on the aperture plane.

Let r, γ (with $r \geq 0$, $0 \leq \gamma \leq 2\pi$) be polar coordinates of $\mathbb{R}^2$, then the generic Zernike polynomial Z_i, $i \geq 0$, is defined on $\mathbb{R}^2$ as follows:

$$Z_i(r,\gamma) = \begin{cases} \sqrt{n+1} R_n^m(r) \sqrt{2} \cos(m\gamma) & \text{if } m \neq 0, i \text{ even} \\ \sqrt{n+1} R_n^m(r) \sqrt{2} \sin(m\gamma) & \text{if } m \neq 0, i \text{ odd} \\ \sqrt{n+1} R_n^m(r) & \text{if } m = 0 \end{cases}$$

where

$$R_n^m(r) = \sum_{k=0}^{(n-m)/2} \frac{(-1)^k (n-k)!}{k! \left(\frac{n+m}{2} - k\right)! \left(\frac{n-m}{2} - k\right)!} (r)^{n-2k}$$

and n, m are two integers uniquely identified by i. Table I summarize the relation[2] between i, n, m and provides some examples of Zernike polynomials. The integer n, with $n \geq 0$, is called the level of the polynomial. Notice that $m \leq n$ and if i_1, i_2 are on the same level then $n - m_k$, $k = 1, 2$ are even and $m_1 - m_2$ is even.

[2]Notice that some authors use different conventions for the relation between n, m and i. We used the Noll convention [8].

Zernike polynomial	i	n	m
$Z_1 = 1$	1	0	0
$Z_2 = 2r\cos\theta$	2	1	1
$Z_3 = 2r\sin\theta$	3	1	1
$Z_4 = \sqrt{3}(2r^2-1)$	4	2	0
$Z_5 = \sqrt{6}r^2\sin(2\theta)$	5	2	2
$Z_6 = \sqrt{6}r^2\cos(2\theta)$	6	2	2
$Z_7 = \sqrt{8}(3r^2-2r)\sin(\theta)$	7	3	1
$Z_8 = \sqrt{8}(3r^2-2r)\cos(\theta)$	8	3	1
$Z_9 = \sqrt{8}r^2\sin(3\theta)$	9	3	3
$Z_{10} = \sqrt{8}r^2\cos(3\theta)$	10	3	3

TABLE I
EXAMPLES OF ZERNIKE POLYNOMIALS AND THEIR INDEXES.

Define $\Pi(\cdot)$ as follows

$$\Pi\left(\frac{r}{R}\right) = \begin{cases} \frac{1}{\pi R^2} & \text{if } r \le R \\ 0 & \text{otherwise} \end{cases}$$

and let δ_{ij} be the Kronecker function

$$\delta_{ij} = \begin{cases} 1 & \text{if } i = j \\ 0 & \text{otherwise} \end{cases}$$

then

$$\int_{\mathbb{R}^2} \Pi\left(\frac{r}{R}\right) Z_i\left(\frac{r}{R},\gamma\right) Z_j\left(\frac{r}{R},\gamma\right) r \; \mathrm{d}r\mathrm{d}\gamma = \delta_{ij}$$

that is the Zernike polynomials forms an orthogonal basis of the continuous region inside the circle of ray R (where R in this case is equal to the telescope aperture's ray). However, since here we are considering the discrete domain $\mathbb{L}$, commonly they are not orthogonal.

Let $z_i = \mathrm{vec}\Big(\big\{Z_i(r,\gamma) \mid r\exp(-j\gamma) \in \mathbb{L}\big\}\Big)$, then using the Zernike polynomials $C = [z_2 \; z_3 \ldots z_{N+1}]$, (5) becomes:

$$\hat{\varphi}(y) = \sum_{i=2}^{N+1} z_i \hat{a}_i = \begin{bmatrix} z_2 & \ldots & z_{N+1} \end{bmatrix} \hat{a}$$

where $\hat{a}$ is still computed with (6).

B. PCA representation

In this section we introduce a representation based on PCA. Principal component analysis yields an alternative set of bases: It is well known that if the second order statistics of the signal are known, the PCA bases take to the best (minimum error variance) reduced order representation of the signal.

The signal φ is a zero-mean $\mathbb{L}$-dimensional (wide-sense) stationary random vector, that is $\varphi \sim (0, \Sigma_\varphi)$. Then there exists a unitary[3] matrix $U = \begin{bmatrix} u_1 & \ldots & u_N & \ldots & u_{|\mathbb{L}|} \end{bmatrix}$, such that

$$\Sigma_\varphi = U\Lambda U^T$$

with

$$\Lambda = \mathrm{diag}(\lambda_1 \; , \; \lambda_2 \; , \; \ldots \; , \; \lambda_{|\mathbb{L}|}), \; \lambda_1 \ge \cdots \ge \lambda_{|\mathbb{L}|} \ge 0.$$

[3]Since $\Sigma_\varphi \in \mathbb{R}^{\mathbb{L}\times\mathbb{L}}$, $UU^T = U^TU = I$.

Moreover since φ is orthogonal to c_0 it is simple to prove that $\lambda_{|\mathbb{L}|} = 0$. Thus $\begin{bmatrix} c_0 & u_1 & \ldots & u_N & \ldots & u_{|\mathbb{L}|-1} \end{bmatrix}$ is a basis of $\mathbb{R}^{\mathbb{L}}$.

Define $x = U^T\varphi$, then $\mathbf{E}[xx^T] = \Lambda$. x is called the vector of principal components of φ, while U is the set of orthogonal bases associated to the principal components. Principal components provide an optimal (minimum error variance) dimensionality reduction step: Let $\hat{\varphi}$ be the random vector reconstructed from φ by means of the first N principal components $\hat{\varphi} = \begin{bmatrix} u_1 & \ldots & u_N \end{bmatrix} x_N$, with $x_N = \begin{bmatrix} x(1) & \ldots & x(N) \end{bmatrix}$. Then

$$\mathbf{E}\|(\varphi - \hat{\varphi})\|^2 = \mathbf{E}(\varphi - \hat{\varphi})^T(\varphi - \hat{\varphi}) = \sum_{i=N+1}^{|\mathbb{L}|-1} \lambda_i.$$

It is simple to prove that this is the minimum distance between φ and a vector $\hat{\varphi}$ given by linear combination of N bases.

Fig. 3 shows the first Zernike polynomials and the first PCA bases computed for a turbulence where $L_0 = 16$m and $r_0 = 1.5$m. Since the piston mode Z_1 is useless for adaptive optics purposes, it is not shown.

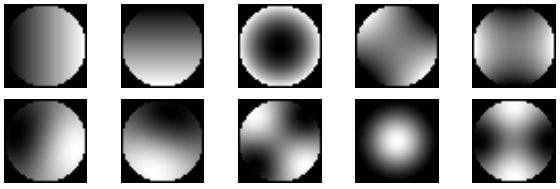

Fig. 3. Top row: Zernike polynomials Z_2, Z_3, Z_4, Z_5, Z_6. Bottom row: The first five PCA bases computed for a particular turbulence. $L_0 = 16$m, $r_0 = 1.5$m, telescope diameter $D = 8$m.

V. COMPARISON BETWEEN PCA AND ZERNIKE REPRESENTATIONS

We can summarize the algorithm of the adaptive optics system as follows:

1) estimate the current turbulent phase, as described in Section III;
2) compute the correction contribution to obtain the compensated phases;
3) control the deformable mirrors, i.e. apply to the system the new correction phases.

The adaptive optics system provides a valuable improvement in telescope performances: Thus both phase reconstruction (step 1 of the algorithm) and feedback computation (step 2) should be as accurate as possible. For this reason we shall use a large number of bases, N, to represent accurately the phases. On the other hand, the high sampling frequency and the need of an almost immediate phase correction make the computational time a stringent design parameter. From (8), the computational complexity of the phase reconstruction step is $O(n|\mathbb{L}|)$. A common assumption [9] [7] is that of having a linear relation between a and the input u of the actuators : $u = Ga$. Let m be the number of actuators, then the computational complexity of step 2) is $O(nm)$. Thus N

is linearly proportional to the running time for computing both the phase reconstruction step and the feedback u: Hence N should be taken small. Since N cannot be chosen simultaneously large and small, this translates in the need of a good set of bases to represent the signal.

As long as representations are compared on the variance of the projection error η, PCA provides by construction the best bases. Here we investigate what happens when considering the representation error e.

We report here the results of some simulations: We compare Zernike polynomials and PCA bases among three possible turbulence conditions. In each case we compute (9), ranging the number of bases from $N = 65$ to $N = 209$. Moreover we compute performances modeling the measurement process both as a spatial mean and as a Shack-Hartmann sensor (as described in Section III). In figures we plot the percent error energy, i.e. $\mathbf{E}[\|e\|^2]/\mathbf{E}[\|\varphi\|^2] \cdot 100$.

The results reported in Fig. 4 are obtained setting the values of the parameters to: $r_0 = 1.5$m, the telescope aperture diameter $d = 8$m, $p_s = 0.2$m, $|\mathbb{L}_{sp}/\mathbb{L}| = 9$, $SNR = 4$. Different values for L_0 are explored: $L_0 = 16$m, $L_0 = 12$m, $L_0 = 20$m.

Finally in Fig. 5 we explore the case of very noisy measurements: $SNR = 2$. The other parameters are set to: $L_0 = 16$m, $r_0 = 1.5$m , $d = 8$m, $p_s = 0.2$m, $|\mathbb{L}_{sp}/\mathbb{L}| = 9$.

VI. CONCLUSIONS

In this paper we have reported a comparison between Zernike polynomials and PCA bases as representations of the turbulent phase measured on telescope lens.

Our simulations have shown that the Zernike representation has to use a significatively larger number of bases to obtain the same performances of PCA bases. Even if our comparison here is only static, i.e. without exploiting the dynamic of the turbulence, in [3] we have considered a dynamic framework: This confirms the encouraging results obtained for the static case.

We are confident that the use of PCA bases instead of Zernike polynomials should allow a significative saving in terms of running time or an improvement in performances.

VII. ACKNOWLEDGMENTS

We are pleased to acknowledge the colleagues of the ELT Project, in particular Dr. Michel Tallon at CRAL-Lyon, and Dr. Enrico Fedrigo at ESO-Munich, for their precious help in supporting us with the astronomical view of the problem, and for many valuable and enjoyable discussions on the subject.

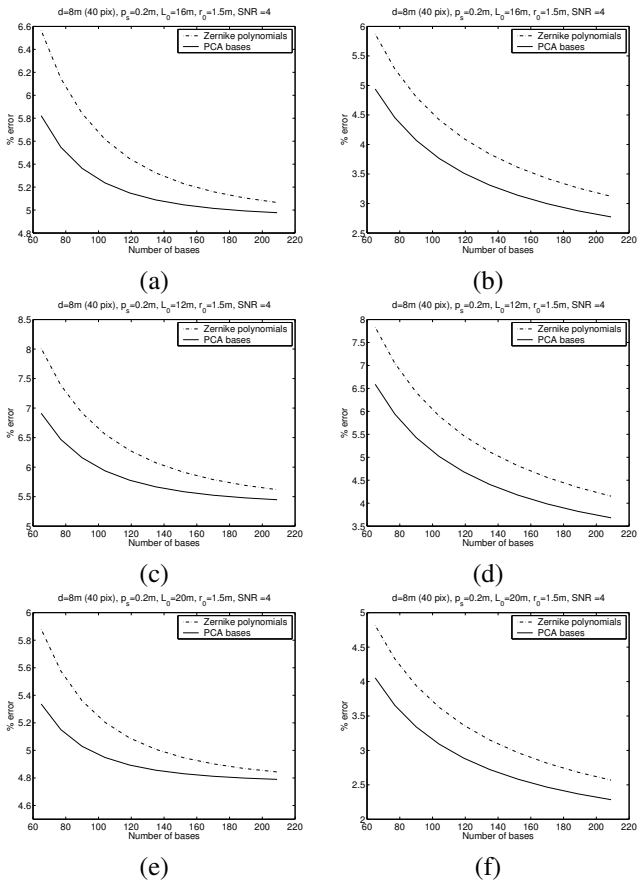

Fig. 4. In solid line the representation errors for PCA bases, in dashed line those for Zernike polynomials. Both spatial mean (in (a), (c), (e)) and Shack-Hartmann (in (b), (d), (f)) methods of measurement are simulated. Different values of L_0 are explored: $L0 = 16$ in (a) and (b), $L0 = 12$ in (c) and (d), $L0 = 20$ in (e) and (f). $SNR = 4$.

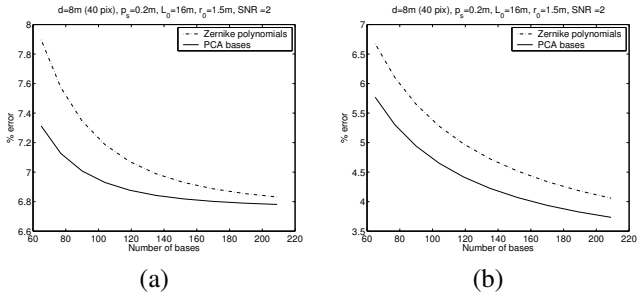

Fig. 5. In solid line the representation errors for PCA bases, in dashed line those for Zernike polynomials. Both spatial mean (in (a)) and Shack-Hartmann (in (b)) methods of measurement are simulated. $L0 = 16$, $SNR = 2$.

REFERENCES

[1] Astronomical seeing. *from Wikipedia, the free encyclopedia [Online]*, 2007.

[2] Zernike expansion of kolmogorov turbulence. *from the Berkeley Astronomy website [Online]*, 2007.

[3] A. Beghi, A. Cenedese, and A. Masiero. Atmospheric turbulence prediction: a pca approach. In *CDC 2007*.

[4] R. Conan. *Modelisation des effets de l'echelle externe de coherence spatiale du front d'onde pour l'observation a haute resolution angulaire en astronomie*. PhD thesis, Université de Nice Sophia Antipolis Faculté des Sciences, 2000.

[5] D.L. Fried. Least-square fitting a wave-front distortion estimate to an array of phase-difference measurements. *Journal of the Optical Society of America*, 67.

[6] D.L. Fried. Statistics of a geometric representation of wavefront distortion. *J. Opt. Soc. Am.*, 55:1427–1435, 1965.

[7] B. Le Roux. *Commande optimale en optique adaptative classique et multiconjuguee*. PhD thesis, Université de Nice Sophia Antipolis, 2003.

[8] R.J. Noll. Zernike polynomials and atmospheric turbulence. *Journal of the Optical Society of America*, 66(3):207–211, March 1976.

[9] F. Roddier. *Adaptive optics in astronomy*. Cambridge university press, 1999.